









Differential Diagnostics of Endometrial Cancer/Atypical Glandular Hyperplasia: Electron Microscopic Examination

Mahira Firudin kizi Amirova^{*1}, Safarova Samira İlyas qızı², Gulnara Alisha qizi Jafarova¹, Ellada Eldar qizi Huseynova¹, Sabina Rafiq Qizi Guliyeva¹, Samira Arif qizi Baghirova¹, Fereh İsmayil qızı Mammadova¹ and Ali Nadir Aliyev¹

¹Azerbaijan Medical University, Department of Biochemistry, Azerbaijan

²Azerbaijan Medical University, Department of Oncology, Azerbaijan

Article Info

Received: 06 July 2025

Revised: 16 November 2025

Accepted: 12 December 2025

Published: 30 December 2025

Keywords

Atypical Glandular
Hyperplasia
Endometrial Cancer
Malignancy
Proliferation
Electron Microscopy



ABSTRACT

This study highlights the significance of electron microscopic analysis in diagnosing proliferative changes associated with endometrial cancer, since the cytological investigations utilizing electron microscopy are of considerable scientific and clinical value for identifying atypical cells. Purpose of the study was to assess the diagnostic importance of electron microscopic examination in detecting proliferative alterations in endometrial cancer. Materials and Methods. The research involved 132 patients diagnosed with endometrial adenocarcinoma (main group) and 35 patients with atypical glandular hyperplasia (control group). Surgical specimens obtained from patients with uterine cancer were submitted to the electron microscopy laboratory for examination using both light and electron microscopy techniques. Findings. Atypical glandular hyperplasia is primarily characterized by the formation of basement membrane invaginations, mitochondrial swelling, roughened mitochondrial cristae, and engorgement of interstitial stromal capillaries. In well-differentiated adenocarcinomas, some cells exhibited structural deformation of desmosomes and a reduction in their number. In G2-grade tumors, the number of desmosomes further decreased, while in G3 tumors, the few desmosomes present showed complete disintegration. Less than 20% of cells in well-differentiated adenocarcinomas demonstrated degradation of desmosomes, accompanied by mild nuclear deformation, mitochondrial swelling, and partial fragmentation of mitochondrial cristae. In poorly differentiated tumors, over 50% of cells exhibited complete desmosomal degradation, marked nuclear polymorphism, and total fragmentation of mitochondrial cristae. Conclusion. The findings underscore the utility of electron microscopy in evaluating the morphological features of endometrial tissue, aiding in the prediction of proliferative disease progression in patients.

1. INTRODUCTION

Rising consumption of alcohol and tobacco, coupled with vitamin imbalances, contributes to an annual global increase of up to 200,000 new endometrial cancer cases and approximately 50,000 deaths. In 2020 alone, the GLOBOCAN database recorded over 417,000 new cases and 97,370 deaths worldwide, underscoring the significant public health burden posed by this disease [1-5]. Despite important strides in oncology, key challenges remain unresolved in the field of oncogynecology [6].

As symptoms in uterine cancer frequently emerge prior to menopause, accurate and timely

diagnosis is essential for effective treatment of proliferative and malignant endometrial changes [6]. Understanding the pathogenesis of benign versus malignant proliferative processes in the endometrium is a priority in contemporary oncology. Hyperplastic endometrial changes are often precursors to neoplastic transformation, with reported progression rates from atypical glandular hyperplasia to carcinoma ranging from 29 % to 52 % in recent studies [7, 8]. Other analyses suggest a progression risk between 23 % and 40 % [9, 10], emphasizing the clinical importance of early identification and intervention.

Proliferative alterations in the endometrium including simple and atypical hyperplasia as well as

^{*}Corresponding author

How to cite this article

*e-mail: gerayelmira@gmail.com
ORCID ID: 0000-0001-5598-6995

Research Article/ DOI: 10.5281/zenodo.18047637

Amirova, A., Samira, S., Jafarova, G., Huseynova, E., Guliyeva, S., Baghirova, S., Mammadova, F., & Aliyev, A. (2025). Differential Diagnostics of Endometrial Cancer/Atypical Glandular Hyperplasia: Electron Microscopic Examination. *Int. J. Digital Health & Patient Care*, 2(2), 71-78. *Int. J. Digital Health & Patient Care*, 2(2), 71-78.

frank endometrial carcinoma are accompanied by degenerative changes in the endometrial lining, including glandular atrophy, structural breakdown, and nuclear complex destruction. These processes facilitate the emergence of poorly differentiated intraepithelial neoplasms and malignant cells [11, 12].

Early detection of endometrial cancer (EC) is critical for selecting effective treatment strategies. Consequently, the use of minimally invasive diagnostic tools has attracted significant attention. In routine clinical settings, endometrial sampling via mucosal cytology and subsequent histopathological examination remains the gold standard for evaluating abnormal proliferative changes [13]. Among cytological methods, electron microscopy-based cytopathology is particularly valuable for identifying atypical cellular phenotypes with both academic and clinical impact [14, 15].

The prognosis and recurrence risk of EC are determined by factors such as patient age, tumor stage, histological subtype, and grade, which denotes the degree of differentiation and biological aggressiveness [16]. Detailed morphological studies, particularly at the ultrastructural level, may significantly enhance the accuracy of tumor grading and thereby refine prognostic assessment [17].

The objective of this study was to evaluate the diagnostic value of electron microscopic examination in identifying proliferative alterations associated with endometrial cancer.

2. MATERIALS AND METHODS

2.1. Participants

The study population included a main cohort of 132 patients with histologically confirmed endometrial adenocarcinoma and a control group of 35 patients diagnosed with atypical glandular hyperplasia (AGH). Patient ages ranged from 39 to 76 years, with a mean age of 49.6 ± 2.7 years. Both groups presented with non-specific complaints, including abnormal uterine bleeding (bloody or whitish-gray discharge) and lower abdominal pain. Patients with non-resectable tumors, those receiving neoadjuvant chemotherapy or radiotherapy, individuals with distant metastases, patients presenting with recurrent disease at initial consultation, and those diagnosed with concurrent ovarian, vulvar, or other gynecologic malignancies - as well as extragenital tumors - were excluded from the study.

2.2. Research process

This study was conducted jointly at the Oncology Clinic of Azerbaijan Medical University (AMU), the electron microscopy laboratory of the

Research Center, and the Department of Histology, Cytology, and Embryology at AMU. The investigation utilized both surgical specimens and archived clinical data from patients diagnosed with endometrial adenocarcinoma. A mixed-method approach combining retrospective and prospective analysis was employed. Findings from clinical assessments, ultrasonography, histopathology, and electron microscopy were systematically recorded and analyzed. Among the 132 cancer patients, tumor localization was as follows: 35 patients (26.5%) had tumors in the upper uterine corpus, 27 (20.4%) in the lower third, and 31 (23.5%) in the central uterus region. In 18 patients (13.6%), the uterine cavity was completely occupied by the tumor, while cervical involvement was observed in 21 patients (15.9%). In addition to ultrasonography, 87 patients underwent pelvic MRI. Myometrial invasion was confirmed in 74 cases, and cervical invasion was detected in 13 cases. MRI also indicated regional lymph node metastasis in 9 patients (10.3%). Tissue samples (1.5 cm) containing all uterine wall layers, including both pathologic lesions and unaffected regions, were collected during surgery. These specimens were fixed in a solution of 2.5% paraformaldehyde, 4% sucrose, and 0.1% picric acid, prepared in 1.0 M phosphate buffer (pH 7.4), and sent to the electron microscopy laboratory for further processing.

Semithin (1 μ m) sections were prepared using a Leica EM UC7 ultramicrotome. Ultrathin sections were examined using a JEM-1400 transmission electron microscope (JEOL, Japan) operated at 80–120 kV. Electron micrographs were captured using Veleta digital cameras located at both lower and lateral ports. Morphometric analysis of cellular and tissue structures (e.g., length, diameter, surface area, form factor) was performed using "The TEM Imaging Platform" software (Olympus Soft Imaging Solution GmbH, Germany). Micrographs and electronograms in TIFF format were analyzed semi-automatically. Quantitative data obtained were subjected to statistical analysis using various methodologies: variation statistics via the Mann-Whitney U-test, discriminant analysis using Pearson's Chi-square test, and regression analysis using the Kaplan-Meier method with the Log-Rank (Mantel-Cox) test. All statistical computations were performed using Microsoft Excel 2016 and SPSS version 22.

2.3. Data collection techniques

Clinical information was obtained through detailed anamnesis, including both short- and long-term treatment outcomes. All participants underwent comprehensive clinical, laboratory, and instrumental evaluations, which included

gynecological examination, transvaginal ultrasound and endometrial cytology.

3. RESULTS

To enable a comparative evaluation of cellular and tissue architecture at the ultrastructural level, a range of morphological indicators were analyzed. These included characteristics of the plasma membrane, cytoplasmic electron density (distinguishing dark and light cells), intercellular junctions, nuclear morphology, mitochondrial integrity, Golgi apparatus organization, and both the quantitative features and neovascularization patterns of endometrial secretory cells.

A hallmark finding in atypical glandular hyperplasia (AGH) was pronounced swelling of the basement membrane in endometrial epithelial cells, accompanied by the formation of invaginations of variable sizes. These invaginations, distinctly identifiable under electron microscopy, were not observed in cases of glandular polyps or simple hyperplasia, indicating their specificity to atypical or neoplastic transformation.

Ultrastructurally, the endoplasmic reticulum appeared as a narrow, web-like structure composed of closely arranged parallel cisternae. Mitochondria demonstrated close association with the ergastoplasm and were characteristically swollen an early sign of cellular stress or dysfunction. Additionally, elongated cisternae were frequently observed within cells possessing weakly osmiophilic cytoplasmic features. These cisternae exhibited patterns of anastomosis, contributing to the altered ultrastructural landscape observed in atypical and neoplastic endometrial tissues.

Mitochondria in atypical glandular hyperplasia (AGH) exhibit notable morphological alterations, including increased size, enhanced matrix clarity, and distended cristae. These pathological features reflect a disruption in the synthetic and transport functions of the affected cells. One of the prominent histopathological hallmarks of AGH is the engorgement of interstitial stromal capillaries, a change closely associated with increased metabolic activity and altered vascular permeability.

Characteristic ultrastructural features of AGH include invaginations of the basement membrane, mitochondrial swelling, hypertrophic cristae, and vascular dilation within the stroma. Mitochondrial swelling indicates membrane dysfunction and compromised bioenergetic reactions, suggesting elevated energy demands during the pathological process. These mitochondria are predominantly

localized near the basal plasma membrane and often exhibit severely distended cristae.

The Golgi apparatus typically maintains a perinuclear distribution, situated adjacent to the nuclear envelope, and remains structurally intact despite other cytoplasmic alterations. Notably, while endometrial epithelial cells demonstrate significant atypical change including nuclear and cytoplasmic anomalies they largely retain tissue-specific structural organization. Importantly, the basal membrane remains morphologically preserved in most cases of AGH, suggesting a non-invasive profile at this stage of pathology.

Clinical and structural characteristics of the three histological subtypes of endometrial adenocarcinoma well-differentiated, moderately differentiated, and poorly differentiated were analyzed. Based on histological classification, the well-differentiated subtype (G1) was observed in 53 patients (40.2%), the moderately differentiated subtype (G2) in 40 patients (30.3%), and the poorly differentiated subtype (G3) in 39 patients (29.5%) ($p < 0.05$).

The distribution of patients by clinical stage revealed that the majority were diagnosed at stage I, comprising 73.5% of all cases. More specifically, stage IA was identified in 85 cases (64.4%), stage IB in 28 cases (21.2%), stage II in 9 cases (6.8%), stage IIIA in 6 cases (4.6%), and stage IIIC in 4 cases (3.0%).

When correlating disease stage with patient age, stage I was predominant across all age groups. However, a significant increase in the frequency of stage II and III diagnoses was observed with advancing age. In women of reproductive age, stages II and III were recorded in only 7.1% of cases, whereas in women over 50 years of age, these advanced stages were present in 30.9% of cases ($p < 0.05$).

Electron microscopic analysis of endometrial samples obtained via cytochoectomy revealed notable alterations in glandulocyte morphology, including variations in shape, size, and ultrastructural organization. Changes were observed in the number and architecture of cellular organelles, intercellular junctions, and the structural adaptations of secretory cells responsible for maintaining hemostasis within the endometrial lining during malignant transformation. These ultrastructural modifications are characteristic of endometrial adenocarcinomas and were systematically classified in the context of tumor differentiation and clinical staging.

To enable a comparative analysis of cellular and tissue structural abnormalities at the ultrastructural level, a set of defined morphological indicators was employed. The identified alterations

associated with atypical and neoplastic processes encompassed modifications in the plasma membrane, the presence and distribution of dark and light cells, the integrity of intercellular junctions, nuclear morphology, mitochondrial

structure, Golgi complex configuration, and both the quantitative parameters and neovascularization characteristics of secretory endometrial cells (Fig.1).

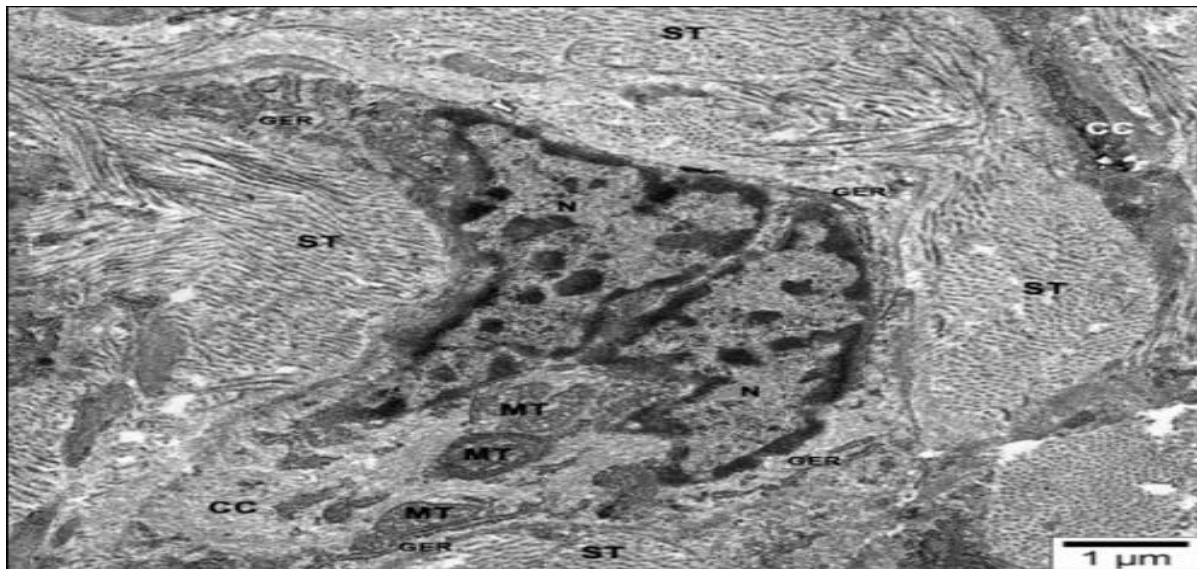


Figure 1a. Ultrastructural features of poorly differentiated endometrial adenocarcinoma (Transmission Electron Microscopy, scale bar = 1 μ m).

Markedly atypical glandular epithelial cells within a poorly differentiated endometrial adenocarcinoma. Numerous pleomorphic nuclei (N) with irregular contours and prominent nucleoli are seen, indicative of nuclear atypia and high-grade malignancy. The cytoplasm contains enlarged mitochondria (MT) with disrupted cristae, signifying mitochondrial dysfunction and altered energy metabolism. The granular endoplasmic reticulum

(GER) is partially degranulated, and cytoplasmic condensation (CC) is evident along the basal and lateral surfaces. Intercellular contact zones appear indistinct, reflecting the loss of desmosomes and compromised cellular adhesion. Stromal tissue (ST) surrounds the neoplastic cluster, with notable separation from the tumor mass, consistent with stromal invasion and architectural disorganization.

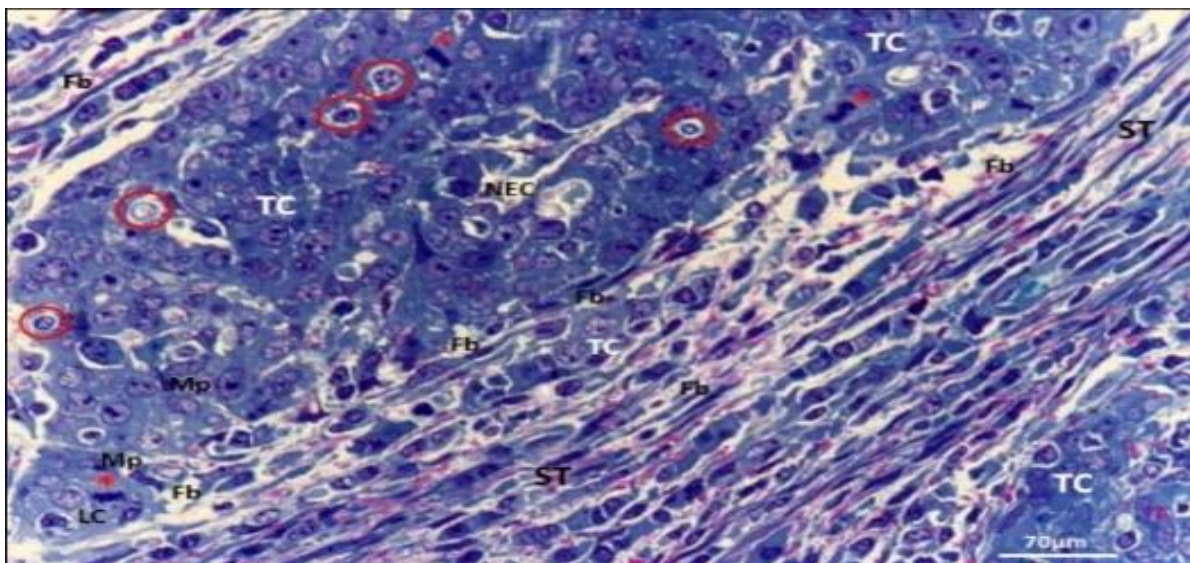


Figure 1b. Light microscopy of poorly neoplasm (Toluidine Blue staining, scale bar = 70 μ m).

A dense, disorganized tumor cell (TC) population infiltrating the stromal tissue (ST). Numerous fibroblasts (Fb) are distributed

throughout the fibrotic stromal compartment, indicating a reactive desmoplastic response. Many tumor cells exhibit signs of necrosis (NEC),

cytoplasmic vacuolization, and nuclear pyknosis. Multiple mitotic figures (circled in red) are identified, reflecting heightened proliferative activity. Multinucleated and mitotically active cells (Mp) are frequently seen alongside lymphocytic clusters (LC), suggesting immune infiltration. The overall tissue architecture is severely disrupted, with indistinct cell borders and diffuse necrotic zones, consistent with a poorly differentiated tumor phenotype.

Moderately differentiated endometrial adenocarcinomas have been identified in 30.3% of patients, with a reported 5-year survival rate of 85%. Ultrastructural analysis revealed the presence of small mitochondria with densely packed matrices situated between the membranes of the ergastoplasm. These mitochondrial matrices contained osmiophilic granules and sparse cristae. The nuclei exhibited irregular, serrated contours, indicative of nuclear atypia. Mitochondria were frequently observed in close proximity to the variability in the morphology of organelles associated with cellular metabolism.

In contrast, poorly differentiated endometrial adenocarcinomas (G3) were diagnosed in 29.5% of patients, with a corresponding 5-year survival rate of 64.1%. Electron microscopic examination revealed that one of the most prominent

plasma membrane, and changes in matrix coloration reflected the anastomosing configuration of cristae arranged in multiple perpendicular orientations.

At the cellular contact zones, complex interdigitations and specialized junctional formations were noted. A marked reduction in the number of desmosomes and associated surface plaques was observed, leading to weakened intercellular adhesion. This loss of structural cohesion was reflected in the infiltration of tumor cells into the surrounding stromal compartments near the primary neoplastic site. Basal regions of cancer cells displayed fragmentation, and the endoplasmic reticulum demonstrated signs of degranulation. Collectively, these ultrastructural changes in moderately differentiated adenocarcinoma point to disrupted intracellular metabolic processes, manifesting as significant

cytoplasmic features in atypical cells was the presence of multivesicular bodies, composed of elements derived from the endoplasmic reticulum (Fig. 2). These findings suggest profound intracellular reorganization and endomembrane system disruption characteristic of high-grade malignancy (Table 1).

Table 1. Comparative ultrastructural and clinical features of moderately vs. poorly differentiated endometrial adenocarcinomas

Parameter	Moderately Differentiated (G2)	Poorly Differentiated (G3)
Prevalence among patients	30.3%	29.5%
5-year survival rate	85.0%	64.1%
Mitochondrial features	Small, dense matrix; located near plasma membrane; contain osmiophilic granules and few cristae	Cristae are less defined; mitochondria structurally degraded
Cristae Organization	Anastomosed, arranged perpendicularly	Severely disrupted, fragmentation common
Nuclear Morphology	Rough, jagged nuclear contours	Marked nuclear polymorphism and irregularity
Endoplasmic reticulum	Degranulated; narrow cisternae	Multivesicular bodies dominate cytoplasm
Golgi Apparatus	Perinuclear position; preserved	Frequently distorted/displaced
Intercellular contacts	Reduced Desmosomes; interdigitations present; weakening of adhesion	Severe Degradation of desmosomes; loss of intercellular integrity
Stromal invasion	Tumor cells infiltrate stroma near primary lesion	Extensive stromal invasion and disorganization
Basal membrane	Basal regions Fragmented; basement membrane typically intact	Often disrupted/ indistinct
Key Ultrastructural marker	Structural variability of organoids indicating metabolic disorder	Multivesicular bodies composed of ER elements

4. DISCUSSION

The findings of this study underscore the significant diagnostic and prognostic value of electron microscopic analysis in endometrial adenocarcinomas. Beyond its role in differential

diagnosis, electron microscopy serves as a powerful tool for evaluating the biological behavior and metastatic potential of tumor cells by examining intracellular ultrastructures. Importantly, this method complements traditional histological, histochemical, and immunohistochemical

techniques, offering a fundamentally new approach to characterizing tumor aggressiveness [15].

A central observation from our research is the progressive loss of intercellular contacts with increasing tumor grade. The structural integrity of desmosomes, which are critical for cellular adhesion, declines in direct correlation with tumor malignancy. Specifically, while desmosomes are preserved in atypical glandular hyperplasia (AGH), partial deformation is observed in some cells of well-differentiated adenocarcinomas (G1). In moderately differentiated tumors (G2), the number of desmosomes decreases noticeably, and in poorly differentiated adenocarcinomas (G3), desmosomal structures are almost entirely absent. This decline in cell-to-cell adhesion correlates closely with both histopathological grading and clinical progression, emphasizing its prognostic relevance. The widespread dissemination of tumor cells throughout the stroma in low-grade tumors further highlights the loss of intercellular cohesion as a marker of accelerated tumor growth and metastatic potential.

A second critical ultrastructural indicator is the morphology of the nucleus and micronuclei. Nuclear enlargement, the formation of deep and sharply contoured invaginations of the nuclear envelope, and pronounced nuclear polymorphism are all hallmarks of malignancy. In our study, these features were most prominent in G3 tumors, where hypertrophic micronuclei exhibited large, complex fibrillary centers. These nuclear alterations were accompanied by heightened mitotic activity an established ultrastructural signature of aggressive tumor biology and rapid progression.

Mitochondrial architecture represented a third major diagnostic criterion. No significant

Ultrastructural examination of endometrial adenocarcinomas revealed distinct morphological signatures that correspond to varying degrees of tumor differentiation. Notably, the presence and

atypical glandular hyperplasia (AGH), increased in number in well-differentiated adenocarcinomas, and were prevalent in over 50% of the examined area in poorly differentiated (G3) tumors. In several G3 cases, stratified layers of dark cells were observed. Our findings suggest that the abundance of these cells correlates with tumor grade and may serve as both a differential diagnostic and prognostic marker. Furthermore, their prominent localization within zones of stromal invasion implies a contributory role in tumor dissemination.

The electron microscopy data also reveal, consistent with previous research, pronounced ultrastructural remodeling within tumor cells [14, 15]. Specific alterations—such as loss of

structural abnormalities were noted in mitochondria during AGH. However, as the degree of tumor differentiation declined, mitochondria became increasingly swollen, and their cristae displayed progressive degeneration, starting with partial fragmentation. These alterations likely reflect heightened cellular hypoxia and a shift toward aerobic glycolysis (the Warburg effect), both characteristic of advanced-stage carcinogenesis.

An additional notable ultrastructural finding relates to secretory endometrial cells, which may serve as potential prognostic markers. Prior studies have indicated that these cells contribute to endometrial homeostasis under physiological conditions. Our investigation revealed a substantial increase in both the number and secretory activity of these cells in poorly differentiated tumors. At the ultrastructural level, this was evidenced by extensive development of the endoplasmic reticulum network, proliferation of intracellular tubules, and a marked rise in the number of secretory granules. These changes likely represent a compensatory response or adaptation associated with tumor progression and heightened metabolic demand.

Collectively, these observations demonstrate that electron microscopy provides critical insights into tumor cell biology that extend beyond conventional light microscopy. Desmosomal integrity, nuclear morphology, mitochondrial status, and secretory cell activity all emerge as key ultrastructural features with strong diagnostic and prognostic implications in endometrial adenocarcinoma.

distribution of dark cells within the cytoplasm emerged as a novel and potentially significant diagnostic marker. These cells were infrequent in

desmosomal integrity, mitochondrial swelling with cristae fragmentation, nuclear polymorphism, and proliferation of secretory granules correlate with tumor aggressiveness and metastatic potential. While desmosomes remain intact in AGH, their progressive degradation from G1 through G3 tumors parallels increased malignancy and reduced cellular adhesion. These observations align closely with histopathological grading and clinical behavior, reinforcing their value in refining diagnostic precision.

Another pivotal finding concerns nuclear morphology. Features such as nuclear enlargement, irregular invaginations of the nuclear membrane, and hyperchromatic micronuclei with hypertrophic fibrillar centers were strongly associated with

poorly differentiated tumors. These features were frequently accompanied by elevated mitotic activity, underscoring their role as ultrastructural indicators of tumor progression.

The ultrastructural condition of mitochondria likewise offers essential insights into tumor biology, as has been emphasized by other investigators [8, 9]. While mitochondrial structure was preserved in AGH, adenocarcinomas showed a progressive increase in swelling and disruption of cristae, suggestive of hypoxic adaptation and metabolic reprogramming. These changes support the hypothesis that tumor cells increasingly rely on aerobic glycolysis (Warburg effect) as malignancy advances.

Additionally, secretory cells of the endometrium displayed increased activity and organelle proliferation in poorly differentiated tumors. This was evident from the expansion of the endoplasmic reticulum network, increased tubulogenesis, and accumulation of secretory granules. The rise in both the number and activity of these cells may reflect a compensatory or pathological response to the rapidly proliferating tumor microenvironment.

Taken together, these findings align with studies indicating that ultrastructural evaluation through electron microscopy not only improves the differential diagnosis of AGH and endometrial carcinoma but also provides deeper insight into tumor biology at the subcellular level [14, 17]. Importantly, these morphological indicators may contribute to the assessment of tumor behavior, metastatic potential, and therapeutic responsiveness.

5. Conclusion

This study demonstrates that specific ultrastructural features including the frequency of dark cells, integrity of desmosomal junctions, mitochondrial remodeling, and nuclear polymorphism serve as meaningful prognostic markers in endometrial adenocarcinomas. The increased prevalence of dark and secretory cells, combined with a marked loss of intercellular adhesion structures, particularly in poorly differentiated tumors, signifies a higher likelihood of metastasis and a more aggressive clinical course. In contrast, the preservation of these structures in AGH supports their utility in distinguishing benign from malignant lesions.

Our findings strongly support the integration of electron microscopic assessment into the diagnostic workflow for endometrial pathology. By bridging the gap between traditional histology and molecular diagnostics, ultrastructural evaluation provides a unique and underutilized perspective

that may help tailor personalized treatment strategies and improve patient outcomes. Future research should explore the functional implications of these ultrastructural changes and validate their prognostic value in larger, multi-center cohorts.

Conflict of Interest

The authors declare that there are no conflicts of interest relevant to the content of this manuscript.

Ethics Committee

This study followed ethical standards and received approval from the Azerbaijan Medical University [Ethics Council of 05.04.2016, protocol No. N11].

Author Contributions

Study Design, Jafarova GA, Data Collection, Baghirova SA and Mammadova F.I.; Data Interpretation, Jafarova GA and Amirova M.F.; Manuscript Preparation, Jafarova GA and Amirova M.F.; Literature Search, Guliyeva SR. Aliyev AN, conceptualization and visualization. All authors have read and agreed to the published version of the manuscript.

REFERENCES

1. Amirova, M. F., Mammadova, K. R., & Huseynova, E. E. (2020). Cancer development under tobacco, alcohol, and opportunistic microbiota action and its reduction with oleuropein. *Journal of Pathology and Infectious Diseases*, 3(2), 1–3.
2. Amirova, M. F., Huseynova, E. E., Aliyev, A. N., et al. (2025). Impact of vitamin D levels drop on endometria hyperplastic post-menopausal bleeding. *Surgical Clinics and Practice*, 2(1), 1–5. [CrossRef]
3. American Cancer Society. (2025). *Key Statistics for Endometrial Cancer*. Retrieved from <https://www.cancer.org/>
4. Sung, H., Ferlay, J., Siegel, R. L., Laversanne, M., Soerjomataram, I., Jemal, A., & Bray, F. (2021). Global cancer statistics 2020: GLOBOCAN estimates of incidence and mortality worldwide for 36 cancers in 185 countries. *CA: A Cancer Journal for Clinicians*, 71(3), 209–249. [CrossRef] [PubMed]
5. GBD 2019 Collaborators. (2020). Global burden of uterine cancer, 1990–2019: Updated results from the Global Burden of Disease Study.
6. Yang L., Yuan, Y., Zhu, R., and Zhang, X. (2023). Time trend of global uterine cancer burden: an age-period-cohort analysis from 1990 to 2019 and predictions in a 25-year period. *BMC Women's Health*, 23:384. [CrossRef] [PubMed]
7. Giannella, L., Piva, F., Delli Carpini, G., Di Giuseppe, J., Grelloni, C., Giulietti, M., Ciavattini, A. (2024). Concurrent endometrial cancer in women with atypical endometrial hyperplasia: What is the

- predictive value of patient characteristics? *Cancers*, 16(1), 172. [[CrossRef](#)] [[PubMed](#)]
8. Lai, X., Chen, Y., & Wang, J. (2022). Atypical endometrial hyperplasia and risk of endometrial cancer: A multicenter retrospective study. *Frontiers in Oncology*, 12, 892995. [[CrossRef](#)] [[PubMed](#)]
 9. Nicola, G., Chang, A., & Gupta, P. (2024). Concurrent endometrial carcinoma in atypical endometrial hyperplasia: Systematic review and meta-analysis. *International Journal of Gynecological Cancer*, 34(1), 66–72. [[CrossRef](#)] [[PubMed](#)]
 10. Smith, R., Patel, A., & Lee, S. (2022). Global trends in endometrial cancer incidence and mortality from 1990 to 2021. *BMC Women's Health*, 23, 2535. [[CrossRef](#)] [[PubMed](#)]
 11. Nguyen, L. T., Smith, C. A., & Huang, H. (2021). Endometrial intraepithelial neoplasia and early carcinoma: Morphologic insights and clinical implications. *Human Pathology*, 117, 35–42.
 12. Torres Rodríguez, C., Gómez Sánchez, A., & Morales Montes, C. (2023). Nuclear and glandular degeneration in endometrial proliferative lesions: A morphological spectrum. *International Journal of Gynecological Pathology*, 42(3), 180–188.
 13. Sato, M., Yoshida, Y., Watanabe, T., & Suzuki, Y. (2022). Endometrial sampling accuracy and patient outcomes: A comparative study of biopsy methods. *European Journal of Obstetrics & Gynecology and Reproductive Biology*, 269, 150–156.
 14. Zhao, J., Liu, Y., & Wu, N. (2024). Diagnostic utility of high-resolution electron microscopy in endometrial cytology. *Cytopathology*, 35(1), 61–69.
 15. Al Kabsi, A., & Patel, R. (2023). Ultrastructure of atypical endometrial cells on electron microscopy: Implications for early EC detection. *Journal of Women's Health*, 32(2), 190–198.
 16. Li, X., Chen, Y., & Zhang, Z. (2023). Clinicopathologic factors and long-term outcomes in endometrial carcinoma: A nationwide cohort study. *Gynecologic Oncology*, 172(1), 45–52.
 17. Wang, F., & Humphrey, P. A. (2022). Morphologic and molecular correlates of tumor grade in endometrial carcinoma. *Archives of Pathology & Laboratory Medicine*, 146(5), e123–e131.